sewer **i**nspection **a**utonomous **r**obot

D28.9 - Changes and Improvements

SIAR Consortium

IDMind (IDM), PT
Universidad de Sevilla (USE), ES
Universidad Pablo de Olavide (UPO), ES

ECH●RD

Table Of Contents

1. Introduction

For Phase II, a new prototype with adjustable width was designed, built and successfully tested in real sewers in the Mercat del Born area. This platform performed the programmed tests, inspecting the 640m-long track in approximately one hour and a half, which was well below the given time (6 hours). During all of this time, the operator at the base station was able to get real-time control of the platform with real-time visual feedback. It was operated in semi-autonomous mode with the exception of the maneuvers for changing directions whenever a fork was found.

There were some issues regarding the platform that have been pointed out by the reviewers in their evaluation report. Namely, during the execution of the inspection plan the platform fell twice in unrecoverable situations and the operators had to manually recover the platform. This was reflected in the review report as follows.

"1.Scientific and/or technological excellence (relevant to the topics addressed by the call)
The SIAR consortium has made commendable progress since the last evaluation at the end of phase I. The design of the robot has been significantly improved, the addition of the springloaded suspension with variable width has increased the reliability of operation and the versatility of the system. Nevertheless, further improvement to the systems and design are needed to further reduce the likelihood of the robot getting stuck in unrecoverable situations, in particular when taking turns or negotiating obstacles.

The following milestones have been achieved:
Safe and stable start, motion and stop
Simple trajectories
Wall following and following a trajectory in straight line
Ground obstacle observation
Autonomy (duration of continuous operation): 4 hours which is satisfactory.

3. Potential impact through the development, dissemination and use of project results.
The potential impact of the SIAR solutions is high, provided that (i) the robust handling of turns and obstacles is resolved and (ii) priority is given to implementing improvements related to the inspection task and the associated reporting requirements. [...]"

We would like to thank the reviewers for kindly provide us with helpful and constructive comments and also for noticing the improvements that had been carried out in Phase II. They have been obtained in a great extent by performing a great number of field experiments in the area (7 sessions with the robot including the final demo and one communication experiment). We would also like to thank the staff from BCASA for their support during the different experiments.

The SIAR consortium is also aware about the issues to be addressed in Phase III. In this document the feedback gathered from the field experiments and the project reviews in Phase II is being considered to refine the system as a whole. This document summarizes the main actions that are being adopted to improve the robotic platform and its communications during Phase III.

2. Report on the final Demo of Phase II

"Mission execution and Working procedures:

Efficient and adequate. Some safety concerns remain about operating the robot with humans present in the sewer, so safety procedures need further improvement. Strong point is that the robot can be reversed which save a lot of time. The change of axis width allows to get into narrower tunnels but it increases instability when manoeuvring or passing obstacles"

The Phase II ended with a final field experiment that was carried out in the presence of the external reviewers and members of the Echord++ PTDI consortium.

In this section, we describe the operational procedure followed to fulfill the mission. Then, we will point out chronologically the main milestones that were achieved during the mission as well as the issues found. Finally we present an inspection report that was obtained during the execution of the mission. It includes images of areas pointed as interesting by the reviewers or where potential defects on the sewer system were automatically detected and confirmed by the operator.

2.1 Deployment of the repeaters

The operational procedure starts with the definition of the manholes where the communications devices have to be deployed. These devices will be used by the system to provide complete network coverage in the area. The location of the base station and the manhole were also defined.

Three wireless repeaters were deployed in the sewers in manholes by fixing them to the stairs. The base station communication module was carried by one operator inside the sewer and deployed at a fork to improve its coverage. The location of the repeaters that covered the demonstration area, with an approximate longitude of 640 m. is depicted in Figure 2.1. These places were the ones that had been presented in our earlier deliverable D28.6.

With this configuration, the operator was able to receive real-time images from up to 4 cameras (3 in the direction of the advance and the upper camera) simultaneously (RGB and Depth) without significant lag. This allowed safe operation of the platform over all the inspection area.

Figure 2.1: Trajectory of the platform (red line) and visited manholes (marked with yellow stickers) during the final demo of Phase II. Disposition of the repeaters with manhole deployment, depicted as black boxes with gray grippers. Reported defects found during the inspection marked in red exclamation signs.

2.2 Mission execution

Table I summarizes the main mission milestones that were detected and generated in the final demo of Phase II. Figure 2.1 is closely related to Table I, as it represents the output of our localization system in red, the manholes traversed during the experiment and the deployment point of the SIAR platform. The deploy was done in a manhole located at Comercial Street, near the intersection with Ribera Street.

The mission was completed in roughly 1h53min without issues with the exception of an accidental fall at mission time 1760 that was produced while manually operating the robot to get better views of a region of interest and another at the very end of the track. Note that this operation will not be needed in the new version of the prototype, as an additional camera installed on an arm will be available in the final version (see Sections 4.2.3 and 5.2). We want to highlight that the operator was able to traverse all the forks along the track manually without much prior training. The aforementioned camera can also be used to help the operator to perform such maneuvers if needed.

Table I: List of the main milestones of achieved during the final Demo of Phase II (2017/10/17).

Mission time (s)	Type	Description
-1670	Deployment	The robot was deployed at Manhole Comercial 1 at 10h12m16s
0	Start	Start of the mission. The mission started at 10h40m06s
81	Manhole	Passing below Manhole Comercial 2
133	Manhole	Passing below Manhole Comercial 3
150	Fork	Starts Fork Comercial/Passatge
250	Fork	Ends Fork Comercial/Passatge
256	Manhole	Passing below closed Manhole
364	Manhole	Passing below Manhole Comercial 4
532	Manhole	Passing below Manhole Comercial 5
576	Manhole	Passing below Manhole Comercial 6
682	Manhole	Passing below Manhole Comercial 7
747	**Alert 0**	Generated alert with description: Crack
795	Fork	Starts Fork Comercial/Fusina
945	Fork	Ends Fork Comercial/Fusina
1090	**Alert 1**	Generated alert with description: Crack detected. Sediments on the floor
1095	Manhole	Passing below Manhole Fusina 2
1135	Manhole	Passing below Manhole Fusina 3
1214	Manhole	Passing below Manhole Fusina 4
1350	Manhole	Passing below Manhole Fusina 5
1568	Manhole	Passing below Manhole Fusina 4
1760	Fall	Fall while taking close up images of a region of interest
2130	Recovery	Recovery of the platform by the operators
2186	Manhole	Passing below Manhole Fusina 3
2267	Manhole	Passing below Manhole Fusina 2
2300	Fork	Starts Fork Comercial/Fusina
2350	Fork	Ends Fork Comercial/Fusina
2369	Manhole	Passing below Manhole Fusina 1
2589	Fork	Starts Fork Passeig/Fusina
2749	Fork	Ends Fork Passeig/Fusina
2785	Pipe	Passing below pipe
2796	Manhole	Passing below Manhole Passeig 4
3047	Manhole	Passing below Manhole Passeig 3
3316	**Alert 2**	Generated alert with description: Crack right.

3330	Fork	Starts Fork Passeig/Passatge
3480	Fork	Ends Fork Passeig/Passatge
3493	Manhole	Passing below Manhole Passatge 1
3551	**Alert 3**	Generated alert with description: Wall cracked.
3600	Manhole	Passing below Manhole Passatge 2
3670	Manhole	Passing below Manhole Passatge 3
3753	Manhole	Passing below Manhole Passatge 3
3787	Manhole	Passing below Manhole Passatge 2
3859	Manhole	Passing below Manhole Passatge 1
3910	Fork	Starts Fork Passeig/Passatge
3985	Fork	Ends Fork Passeig/Passatge
3994	Pipe	Passing below pipe
4145	Manhole	Passing below Manhole Passeig 2
4239	Manhole	Passing below Manhole Passeig 1
4530	Pipe	Passing below pipe
4550	Fork	Starts double fork Passeig/Ribera
4670	Fork	Ends double fork
4703	Manhole	Passing below Manhole Ribera 3
4741	**Alert 4**	Generated alert with description: crack on the right wall.
4890	Fork	Starts Fork Comercial St./Ribera St.
4917	Fork	Ends Fork Passeig/Passatge
4979	Manhole	Passing below Manhole Ribera 2
5057	Manhole	Passing below Manhole Ribera 1
5641	Manhole	Passing below Manhole Ribera 1
5770	Manhole	Passing below Manhole Ribera 2
5843	Fork	Starts Fork Comercial St./Ribera St.
6030	Fork	Ends Fork Passeig/Passatge
6100	Fall	Fall while arriving to the destination manhole
6109	End	The robot arrived to the manhole were it was deployed at 12h27m12s

All the data gathered during the demo was gathered in a log file of the Robotic Operating System (ROS[1]) with the following content:

- 79.9 GB of total content. 1h53min of total time.
- More than 60k compressed images per camera:
  - Front/Back Full resolution (VGA) RGB & Depth
  - Up camera half resolution RGB & Depth

---

[1] http://www.ros.org http://wiki.ros.org/rosbag

      ○   Down-facing cameras (4 in total) half resolution, Depth only.
- More than 1M of IMU messages and 3M tf messages
- Odometry measures
- Automatically generated trajectories
- Operation mode, SIAR status and Communication status logs

2.3 Inspection results

While the KPIs related to inspection were planned for Phase III, we already deployed some automatic inspection capabilities that were executed in real-time during the demo for Phase II. Particularly, the system was able to detect the section type the robot was traversing at each moment based on the 3D information provided by the sensors of the robot. This processing was made online by the system.

The tested inspection capabilities were also able to automatically highlight potential defects on the galleries. The affected areas were marked in the images automatically, so that the operator could directly inspect the alert and confirm the defect. All data and alerts were recorded by the robot during its execution. At the end of the mission, the operator can generate an inspection report with these data, in which the GIS coordinates of the defects are also marked.

In the demo, the entries of Table I marked as Alert were generated by the operator from potential alerts detected by the system and/or suggestions by the reviewers, that could stop the mission as required to point out some interesting points or defects found at the sewer network. In the remaining of the section we will include images gathered at the different reported locations.

2.3.1 Alert ID 0

Approximate Location: 41.3864371269047ºN, 2.1835667670244º E
Local Time: 2017-10-17 10:52:32

This alert was generated as evident defects on the left wall can be found, as well as sediments on the floor.

Image obtained from the front camera.

2.3.2 Alert ID 1

Approximate Location: 41.3863587638969ºN, 2.18316345992166º E
Local Time: 2017-10-17 10:58:15
This alert was generated as evident defects on the left wall can be found (right with the rear camera).
Images obtained from front camera (left) and rear camera (right).

2.3.2 Alert ID 2

Approximate Location: 41.3864067159017ºN, 2.18443510049748º E
Local Time: 2017-10-17 11:35:21
This alert was generated as evident defects on the left wall can be found (right wall in the rear camera), as well as sediments on the floor.
Images obtained from the rear camera.

2.3.4 Alert ID 3

Approximate Location: 41.3862493148859ºN, 2.18316345992166º E
Local Time: 2017-10-17 11:39:16
This alert was generated as evident defects on the right wall can be found. Image obtained from rear camera.

2.3.5 Alert ID 4

Approximate Location: 41.3856977498308ºN, 2.18497454392256º E
Local Time: 2017-10-17 11:59:06
This alert was generated as evident defects on the right wall can be found, as well as sediments on the floor. Image obtained from front camera (left) and rear camera (right).

3. Communications

"Communication with the robot is satisfactory, as is the repeater system. Working procedures for deployment of repeaters in the manholes can be further optimized to reduce traffic impact."

In Phase II, the team worked in a plan for the automatic deployment of the repeaters using a robotic arm installed on the robot. After the development of the system, we realized there were many drawbacks compared with a manual deployment of the repeaters.

The manual deployment of the repeaters was quick and precise. A team of two workers needs to open the manhole, one of the workers goes inside the gallery and fixes a repeater in one of the steps of the manhole. In the end, the team will need to go down the steps and remove the repeaters from those steps. This was a quick operation that was accomplished by two workers.

In the automatic deployment, the robot had to carry the communications devices, put them on the floor while navigating and retrieve them in the end. This procedure restrains the starting and ending path of the robot and the robot will spend part of the mission's time just deploying and retrieving the repeaters.

During Phase II review meeting, the reviewers suggested that the team should remove the robotic arm and the repeaters from the robot and find a way to speed up the manual repeater's deployment without the need to go inside the manhole. By using the proposed manually deployable repeater, the deployment task can be accomplished by a sole operator.

The next section describes the design of the new manual deployable repeater.

3.1 Design of the Manually Deployable Repeater

The new design allows a quick deployment of the repeaters without the need to go inside the manhole to deploy and fix them inside the sewer. Figure 3.1 shows the new wireless repeater design.

Figure 3.1 - Wireless repeater new design.

The operator that carries the repeater just has to open the manhole cover, adjust the repeaters height to the floor and fix it to the manhole first step or to the manhole cover. It takes less than 2 minutes to deploy and retrieve the repeaters. This way the traffic impact is

reduced. Figure 3.2 on left shows the deployment of the repeater on the manhole steps, on the right shows the same repeater installed on the manhole cover.
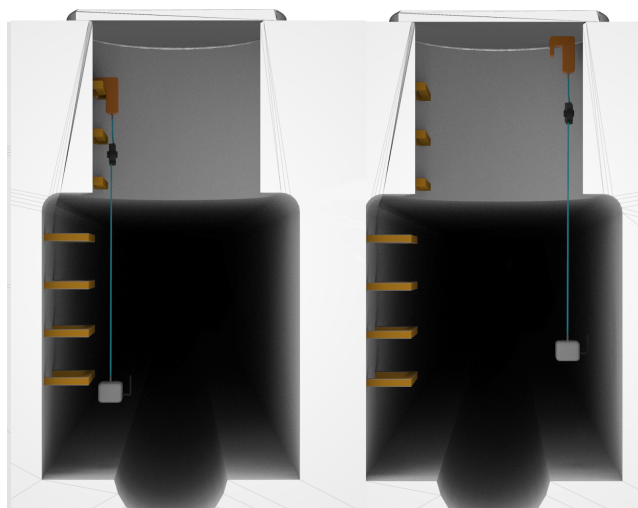

Figure 3.2 - Left: Installation of the repeater on the steps of the manhole.
Right: Installation of the repeater on the manhole cover;

As depicted in Figure 3.1 the system is composed of three parts:

- Top part - includes the battery, the ON/OFF button and the fixing system;

- Middle part - used to adjust the position of the repeater to the sewer gallery floor;

- Bottom part - carries the wireless repeater and a sensor to determine if the repeater is at its optimum position.

The wireless equipment used in Phase II was considered by the reviewers as satisfactory. After evaluating other type of equipments and frequencies, the team was sure that the selected technology is the one to be used in this kind of environment. For this reason, it was decided to continue to use the same devices. Another point to be changed was the increase in the operational time of the repeater. The actual battery is a 11.1V 1450mA LiPo battery with a limited operational time of 2h40. This value should be increased to more than 4h00, to improve the mission operational time for the complete system. For this purpose several types of battery were studied. Table II shows the selected batteries with their sizes and technologies.

Battery Description Manufacture - Type	Capacity (mA)	Oper. Time (h)	Dimensions (H x L x W mm)	Weight (g)
Turnigy - 3S 11.1V Lipo Transmitter pack	1450	2h40	93x40x14	125
Zippy - 3S Flightmax Transmitter pack	2500	4h30	99x31x26	156
Rhino - 3S 11.1V Lipo Low Discharge Transmitter pack	2620	4h50	102x30x36	190

Turnigy - 3S 11.1V Graphene professional pack	3000	5h30	105x35x30	214
Turnigy - 3S 11.1V Graphene professional pack	4000	7h20	107x35x31	296
Turnigy - 3S 11.1V Graphene professional pack	5200	9h40	107x35x51	363

Table II - Study of batteries for the repeaters

In the new design the battery is no longer enclosed with the repeater, and it is installed on the top part. This allowed the team to increase the size and weight of the battery to be used. The size of the battery only depends on the desired operational time, the practical design and ergonomics. For that reason it was created a battery compartment, on the top part, able to house any of the first five batteries of Table II.

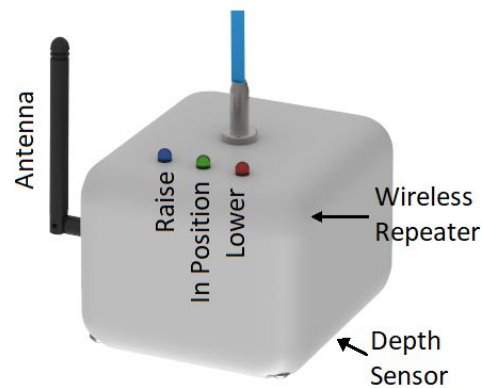The bottom part, shown on Figure 3.3, includes a distance sensor and the wireless repeater.

Figure 3.3 - Repeater bottom part

The distance sensor is an unidirectional micro LIDAR with a detection range of 12m. This sensor will be installed on the bottom of the repeater box, measuring the distance to the sewer floor (not the gutter). The optimum position will be given by a small circuit board that will use the measured distance and activate 3 different LEDs. The blue LED indicates that the system should be raised, the red LED indicates that the system should be lowered and the green is activated when the system is in the right position.

Due to the fact that the wireless repeater consumes a max of 0.5A and the distance sensor consumes 0.13A with peaks of 0.8A we decided not to have both working at the same time. The Top switch will have two working positions:

- Position "I" - powers the repeater power supply and connects the red LED, near the switch;
- Position "II" - powers the distance sensor and connects the green LED, near the switch.

Figure 3.4 shows the repeater top part, which has a shape that allows the system to be hanged on the steps and two magnets on the top to alternatively fix the system to manhole metallic cover.
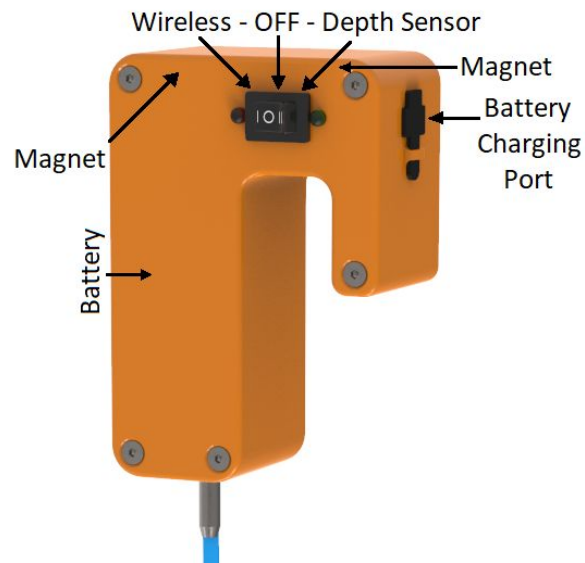
Figure 3.4 - Repeater top part

4. First industrial design (Design V4 IDM)

"[...]. Traction of the wheels should be improved to avoid unrecoverable situations in the turns and intersections. Alternatively, additional measures may be considered to tract correctly under difficulties in the terrain (eg. robot lifting actuator or different size of wheels or larger footprint of the wheels). [...].

Robotic arm: It is recommended that the robotic arm is removed as it adds complexity and costs and adds too little benefit.

Protection of the robot:

Water protection needs to be further improved specifically for the motors. Also material choice is not optimal for the sewer conditions e.g. use of carbon steel bolts instead of stainless steel. It is anticipated that a significant design overhaul will be required to arrive at a robust commercial solution."

During the Phase II evaluation meeting the reviewers pointed the direction to start working for Phase III. The following aspects should be analysed:

- The improvement of the traction system to avoid unrecoverable situations in the turns and intersections;

- The removal of the robotic arm;

- Protection against the environment;

- Protection of the sensible robot parts;

- A better choice of the used materials;

- Adding a camera able to reduce the death areas around the robot and to facilitate the maneuvers;

- Anticipate a significant design overhaul to arrive at a robust commercial solution.

The team decided to redesign the whole robot taking all the best knowledge from the previous phases to achieve a robust commercial solution with enhanced capabilities.

The following subsections describe the actions taken in terms of mechanics and electronics design.

4.1 Mobility

The Phase II robot (SIAR Version 3.0) was analyzed and it was decided to introduce changes in the traction and suspension system while maintaining the possibility to change the width and center of mass of the robot. The new solution increases the ground clearance near the wheels while maintaining the same suspension stroke. The connection between each traction motor and the wheel is maintained with just a small reduction on the pulley

chain. The bottom of the worm gear wheel is now rounded to facilitate the slippage of the robot on the forks' gutter edges (Figure 4.1).

Figure 4.1 - Worm gear protection

The connection between the worm gear box and the arms was inverted, with the linear bearings mounted on the worm gear box while the stainless steel rods with suspension springs are mounted on the wheel arms (Figure 4.2).
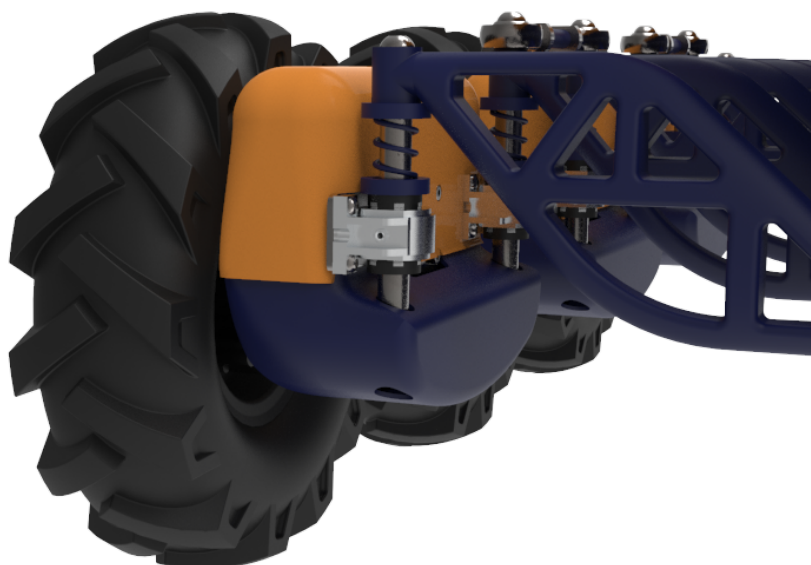

Figure 4.2 - New wheel and arms connection.

The arms design and the way the linear motor actuates were then revised, creating a more attractive and robust system as shown in Figure 4.3.

The linear motor was lifted to be installed between the middle of the bottom and the top central frame. The wheels' arms actuation is now performed in between the top and bottom central frames. This operation increases the central clearance to the floor while protecting these sensible parts.
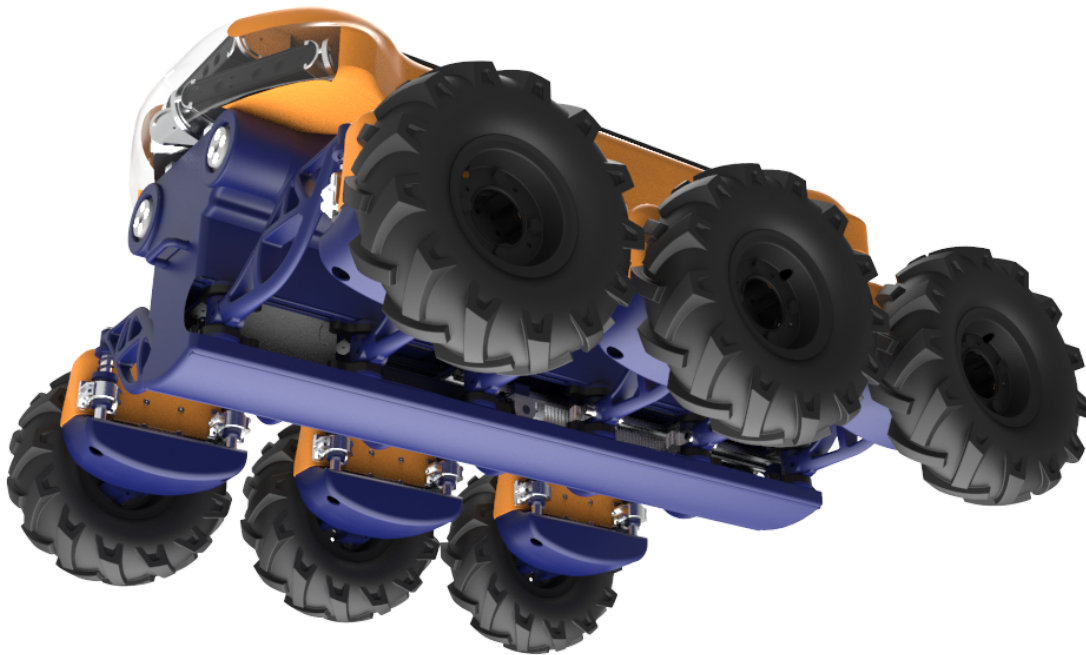

Figure 4.3 - Wheel arms actuation.

The reviewers pointed the need to create a system that could prevent the robot to get stuck in unrecoveral situations or create a system that could recover it from these situations. The team is currently studying a solution to limit the possibility of falling inside the gutter. Two systems are being tested with SIAR v3 robot.

A first solution is composed by a front and rear wheel that will touch the bottom of the gutter (see Figure 4.4). This solution will maintain some pressure on gutter's bottom, maintaining the 6 wheels leveled with the horizontal. In the normal path without forks this system will be the guide of the center of the robot to the middle. If the robot starts to deviate, the pressure on these wheels will make the body to adjust to the center of the gutter.

Figure 4.4 - Photo of SIAR v3 using the first solution in UPO's sewer mock-up

With SIAR v3 prototype, while changing direction on a fork, some of the wheels will lose contact with the horizontal floor and will tend to fall into the gutter, e.g. if the robot is turning left, the 3 left wheels will maintain contact with the horizontal surface, but the right ones will need to lose contact with the horizontal floor to be able to cross to the left side. In this moment, the robot will tend to incline to the left, changing its center of mass to the left wheels that are not touching the horizontal floor, but the slippery gutter edges.

The new system is then projected to support the weight of the robot while crossing the forks, preventing the robot from changing its center of mass from the center, and maintaining the traction on the wheels that are in contact with the horizontal floor.

The second solution is composed by a set of two wheels mounted on the robot's front and rear (see Figure 4.5). This system will use the lateral sides of the gutter to limit the deviation of the robot from the center of the gutter. In the forks, the idea is to use these wheels to force the robot to go up, adjusting the position of the robot to the center of the gutter.

Figure 4.5 - Photo of SIAR v3 using the second solution in UPO's sewer mock-up

The selected idea will have a motorized system, able to rise or lower the wheels depending on the depth of the gutter. A sensor is being studied to determine the depth of the gutter, and with this information calculates what to do with the wheels.

4.2 Payload

The existing payload was analyzed and some changes were performed to improve the reliability of the robot:

- All the repeaters deployment system was taken out of the robot. This includes the removal of the robotic arm and the repeaters' box;

- A new computer was added to increase the image processing;

- The power available for the electronics and motors changed from 230W to 384W, which represents an increase of almost 70% of the available power;

- Inclusion of a robotic arm to control a wide image angle camera to facilitate maneuvers;

- Inclusion of gas sensors, for environmental inspection.

4.2.1. Processing capabilities

Currently, the SIAR robot makes use of a deep neural network in order to automatically detect when the robot passes under a manhole. This information is critical for a good robot localization because it is used as prior to eliminate wrong localization hypotheses. Additionally, we plan to test new deep learning approaches for sewer inspection.

While accurate and powerful, deep learning approaches might need significant computational resources, of course during the network training, but also during network forward-pass in large setups. However, the onboard computer is already highly loaded with all the localization, navigation and perception approaches.

Given such limitations, a new computer (NVIDIA Jetson) will be included into the robot in order to outsource image data processing algorithms based on deep learning approaches. The NVIDIA Jetson is a low-cost and low-power CPU+GPU solution that can be easily installed into the robot. The main benefit of this new computer is the integration of a low-power NVIDIA GPU that can perform the forward-pass of convolutional neural networks at low computational cost.

4.2.2. New Batteries

The current system uses two LiFePO4 12V 18Ah batteries. One of the batteries was used to power all the electronics and the other was used to power the motors system. With the increase of the processing power and sensors there was the need to increase the available power provided by the batteries. As so it was decided to change the battery size to smaller ones that better fit the new design. Meaning, the new design includes four LiFePO4 12V 15Ah batteries. Figure 4.6 illustrates the different sizes of the two batteries.

Figure 4.6 - Left: Old battery; Right: New battery.

The electronic system will be powered by a set of two batteries and the motors system as well. Each set will be the equivalent to a 12V 30Ah battery.

4.2.3. Robotic arm camera

"It is recommended that operator information about position of the wheels and immediate surrounding of the robot will be improved, eg. by adding a wide angle camera."

In Phase II evaluation, the reviewers stated that there was a need to have a camera that could be used to mitigate the death areas around the robot while navigating or crossing the sewer forks, and that could be used to perform inspections of the galleries.

To be able to perform all of these tasks, it was decide to include a camera mounted on a simple robotic arm. This system will be mounted on the robot's top to increase the camera capabilities and to simplify the robotic arm movements. Figure 4.7 shows a simple inspection where the full arm does not need to be fully activated.

Figure 4.7 - Simple Inspection configuration

Figure 4.8 shows the camera in a position that allows to see, at the same time, the robot wheels position and the gutter.

The robotic arm will have springs on the motor joints to provide some stability to the camera image while navigating on the sewer galleries. The same springs will be used to keep the robotic arm in a retracted position, while the robot is been deployed/retrieved from the sewer, or while not in use.

Figure 4.8 - Possible navigation configuration

4.2.4. Gas sensors

In Phase III the robot will be able to measure gases concentrations inside the sewers. For that purpose it was included a Waspmote Pro OEM gas system on the robot. Figure 4.9 shows the acquired Waspmote Pro system.
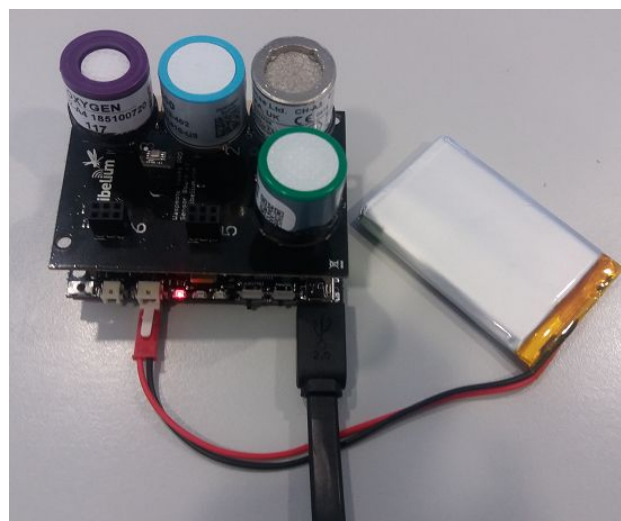

Figure 4.9 - Waspmote Pro OEM gas system

The sensor can measure the following gases:

- Molecular Oxygen (O_2) Gas Sensor [Calibrated]. It will provide the percentage of oxygen on the environment with an accuracy as good as ±0.1% (ideal conditions). It will give an alarm if the percentage drops under 19.5% or if it rises above 23.5%.

- Carbon Monoxide (CO) Gas Sensor for High concentrations [Calibrated]. It will provide the ppm of the CO concentration with an accuracy as good as ±1 ppm (ideal conditions). It will give an alarm if the ppm are above 50 ppm.

- Hydrogen Sulfide (H_2S) Gas Sensors [Calibrated]. It will provide the ppm of H_2S concentration with an accuracy as good as ±0.1 ppm (ideal conditions). It will give an alarm if the ppm are above 5ppm.

- Methane (CH_4) and Combustible gases sensor [Calibrated]. It will provide a measure of LEL methane percentage with an accuracy as good as ±0.15% LEL (ideal conditions). It will give an alarm if the percentage is above 50%.

The system also includes a temperature (ºC), humidity (% RH), pressure sensor (Pa) that will be used to increase the accuracy of the gas sensors. Figure 4.10 shows a datalogin from the sensors. In addition to the gas sensors information previously described, it is also possible to determine the inclination of the board, using an 3-axis accelerometer, the voltage and power level of the battery.

```
++++++++++++++++++++++++++++++++++
Acceleration X: -16 | X angle: -0.9167715072
Acceleration Y: -87 | Y angle: -4.9910416603
Acceleration Z: 1000 | Z angle: 90.0000000000
Battery Level: 85 % | Battery (Volts): 4.0840001106 V
Gas O2 concentration: 20.7667961120 Vol. % - O2 Alarm: OFF
Gas H2S concentration: 0.5267459869 ppm - H2S Alarm: OFF
Gas CO concentration: 0.4259382247 ppm -  CO Alarm: OFF
Gas CH4 concentration: 0.0000000000 % LEL - CH4 Alarm: OFF
Temperature: 25.8799991607 Celsius degrees
RH: 47.8994140625 %
Pressure: 99022.8593750000 Pa
**********************************************
```

Figure 4.10 -SIAR gas sensors datalogin example

4.3 Robot isolation

The robot design includes a protective shell, that protects all the electronics components, sensors, batteries, lights and motors (see Figure 4.11).
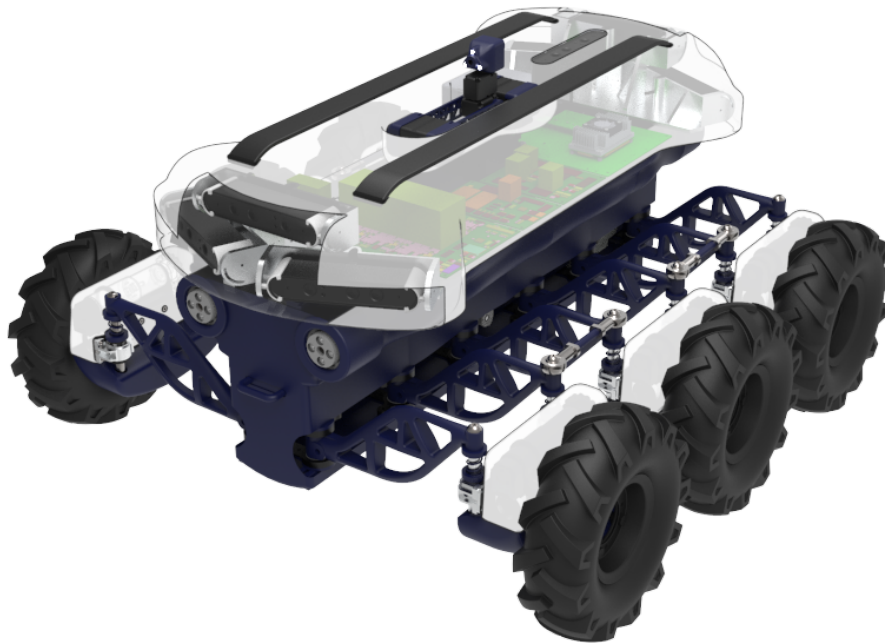
Figure 4.11 - Electronic components position inside the robot.

The RGBD cameras will be installed under a protective transparent polycarbonate that will protect them against the falling water and contact with the sewers walls (see Figure 4.12).
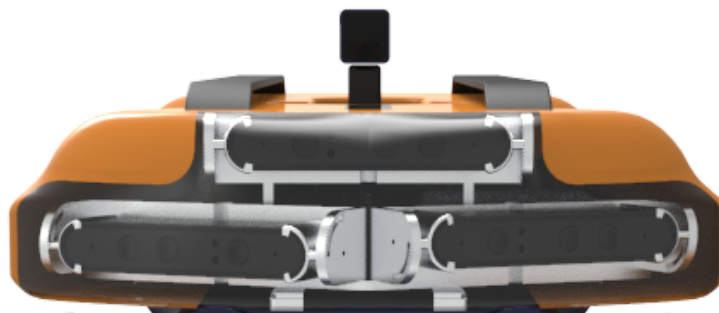

Figure 4.12 - RGBD cameras protection

On top, two aluminium bars were added to facilitate the deployment /retrieval of the robot, on the manhole, preventing the shell from colliding with the manhole walls (see Figure 4.13).

Figure 4.13 - Protective aluminium bars

Also on top, a hole containing the robotic inspection arm camera will prevent the arm and camera from being damaged while the robot passes through the manhole.The motors and motor sensors are now inside a protective and waterproof shell (see Figure 4.14).
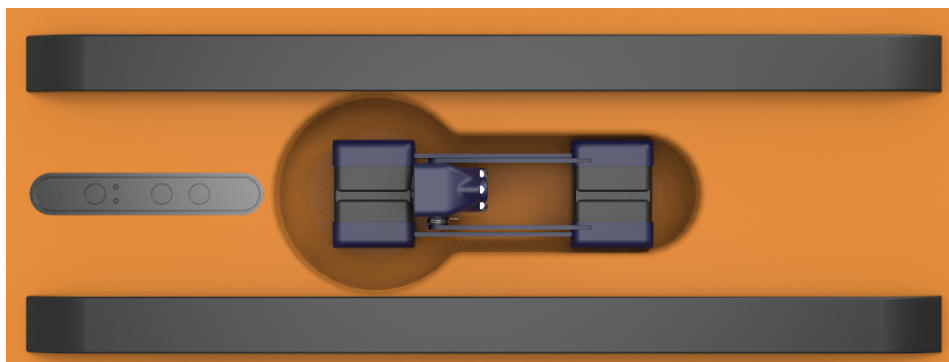

Figure 4.14 - Robotic arm camera container

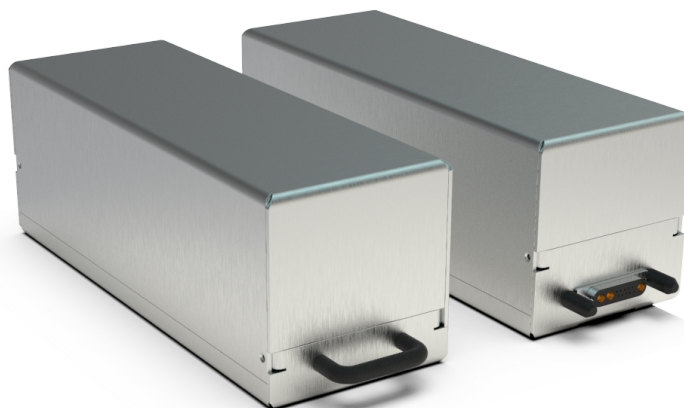Each set of 2 batteries will be isolated and installed in a drawer as shown in Figure 4.15.

Figure 4.15 - SIAR battery sets

The drawer with the batteries will enter the robot in a sliding motion and perform a isolated contact with interior electronics (Figure 4.16). This way the battery changing time will be dramatically reduced.

Figure 4.16 - Battery drawer

The motors power connectors and sensors will enter the main isolated body using IP67 power and signal connectors. The illumination will also be installed on the robots body, inside an IP66 enclosure as shown in Figure 4.17).

Figure 4.17 - Environment robot illumination

To ease the downing and lifting of the system, two eye bolts were fixed to the robot structure, as shown in Figure 4.18.

Figure 4.18 - Worst loading scenario - full robot weight on one wheel (600N)

4.4 Materials

"(...) material choice is not optimal for the sewer conditions e.g. use of carbon steel bolts instead of stainless steel. It is anticipated that a significant design overhaul will be required to arrive at a robust commercial solution."

To protect the robot under the highly corrosive environment of the sewage all exposed steel parts were redesigned to be manufactured in AISI 316L stainless steel. This includes but is not limited to: suspension shafts, gearing, supporting brackets and bolts. Also, high resistant ABS covering shells were designed to better protect the structure and its components. This will not only drastically improve the robustness of the system under the harsh environment but also ease the cleaning processes, making possible the cleaning with just a jet of water.

The camera windows will be coated with a hydrophobic spray that will maintain the windows clean from dirt. This hydrophobic layer will repeal any dirty water that may fall over the camera windows. Figure 4.19 shows a surface where such layer was applied on the right side.
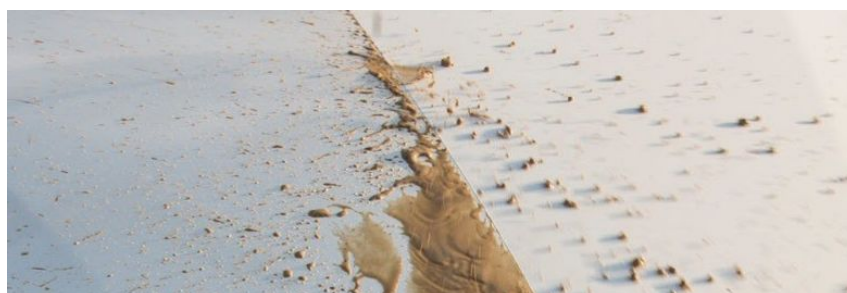

Figure 4.19 - Hydrophobic surface (right side) with mud

To improve reliability and ensure structural integrity, numerous FAE (finite element analysis) were performed in critical components and design and material changes were made

according to results. This was the case, for example, of the new suspension arms, designed in the high performance polymer ULTEM 1010. The arms were tested under the Von Mises yield criteria for a worst case loading scenario, with the results presented in figure 4.20.
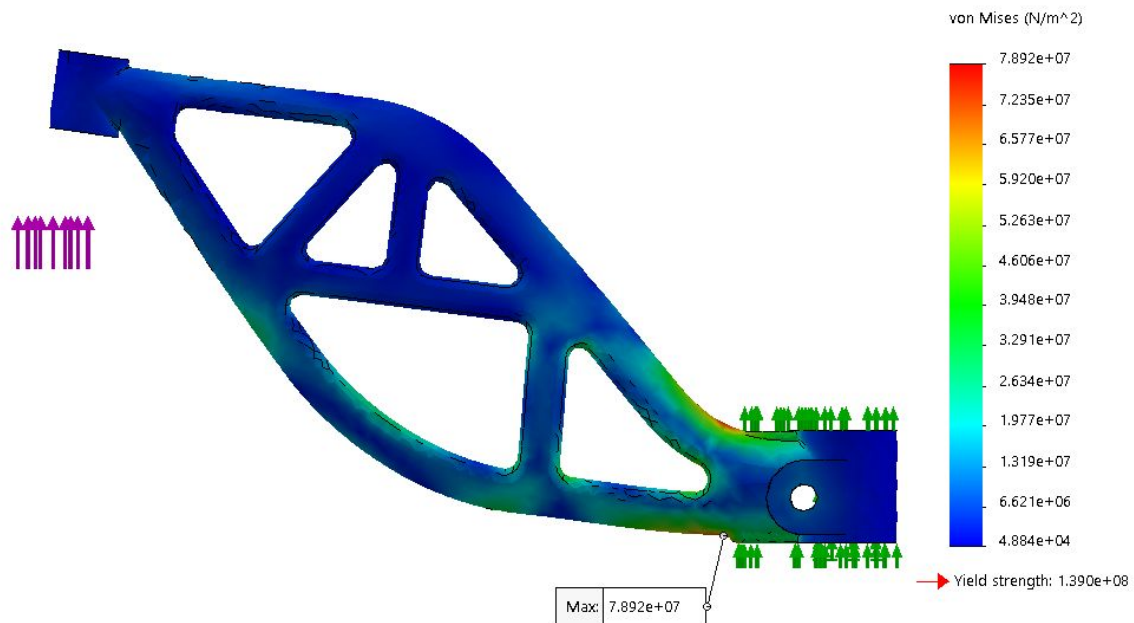

Figure 4.20 - Worst loading scenario - full robot weight on one wheel (600N)

5. Navigation

"Execution of complex trajectories is not robust and needs improvement. Once the robot detects situations that it cannot resolve, it stops and manual mode is needed to resolve the situation. The execution of such manoeuvres is strongly dependent on operator skills, but he has very little information to work with. This results in a high likelihood of the robot getting stuck, as happened repeatedly during the demonstration test. It is recommended that operator information about position of the wheels and immediate surrounding of the robot will be improved, eg. by adding a wide angle camera. Key operational parameters for negotiating bends and obstacles should be studied and used for automating navigation as much as possible."

We agree with the reviewers that the execution of complex maneuvers is a key feature that has to be fulfilled in Phase III. In Phase II, a semi-autonomous mode was designed that was able to guide the platform in straight and curved sections without any issues (please refer to D28.6 Section 5.3.1). In fact, the algorithm was able to transverse forks in some situations as presented in the D28.6, Section 5.3.2. Unfortunately, we found that this procedure was not robust enough for the final demo and we opted to perform these maneuvers manually to improve the reliability of the experiment.

In Phase III, we are performing the following actions to improve the navigation system and achieve the safe navigation in semi-autonomous mode over all the inspection track and to increment the operator awareness in troublesome situations such as forks and presence of steps, to name a few.

1. The addition of a support system that is always in contact with the gutter to avoid the SIAR platform to fall into unrecoverable situations, as presented in Section 4.1.

2. The development of a realistic simulator of the platform in order to test new approaches for robot navigation and to train the operator.

3. The inclusion of an additional camera for better operator awareness during complex maneuvers.

4. The improvement of the semi-autonomous mode to handle obstacles and avoide dead zones.

5.1 Dynamic simulator of the SIAR platform

We developed the algorithms used in the semi-autonomous mode in Phase II by testing them in two real scenarios: a mockup of the sewer that was constructed at the UPO basements which was presented in the Demo of March, 2017 and the real sewers in Barcelona. However, the variety of tracks that are present in a real network are difficult to represent with a mockup and performing experiments in real sewers is costly as it involves not only the mobilization of our personnel but also additional staff from BCASA not to mention the displacement and configuration of the SIAR platform.

In order to reduce costs and also to exhaustively test the algorithms present in semi-autonomous mode we are developing a realistic simulator of the platform that models the main capabilities of our platform. The simulator has been developed with Gazebo[2] simulator that can be easily integrated within ROS. This simulator can be used also for initial training of an operator.

The main characteristics of our simulator are:

- Simulation of the 6 wheel configuration with spring damping system.
- Realistic dimensions, weights and dynamic parameters of the platform.
- Simulation of the width adaptation mechanism.
- Uses the same interfaces as the real platform.
- Realistic simulation of the RGB-D cameras.
- Scenarios obtained by employing the 3D reconstruction of the environment obtained as described in D28.6, Section 6.2.2.
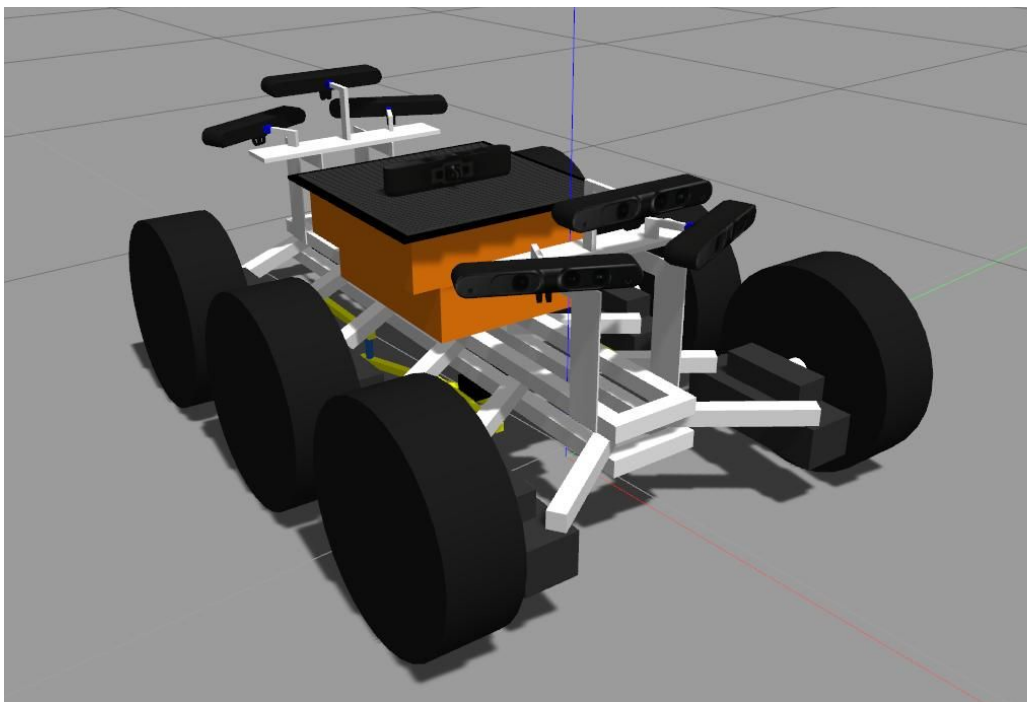

Figure 5.1: Close view of the simulated robot
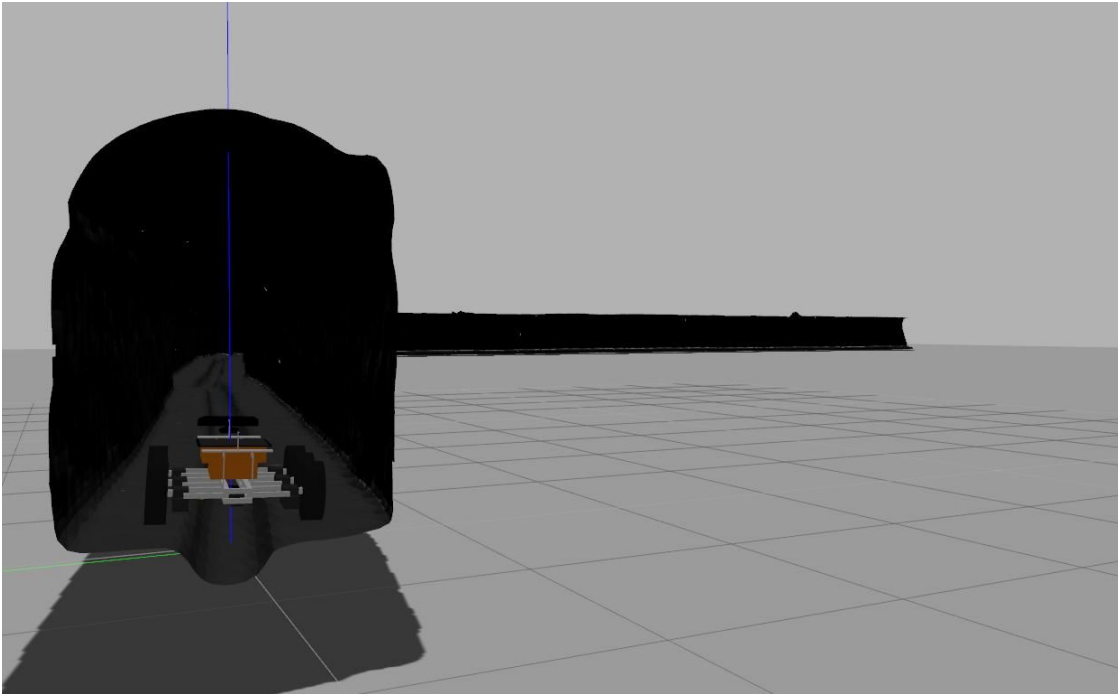
---

[2] http://gazebosim.org

Figure 5.2. Robot navigating into a 3D reconstruction of the real sewers.

We want to highlight the fourth point of the characteristics. The system will share the interfaces with real SIAR platform. In this way, we are able to test the high level systems such as the navigation, localization and inspection directly in simulation without the need of an adaptation layer or configuration changes. This is usually referred as Software in the Loop (SITL) simulation that is widely used in robotics' developments and allows us to develop the algorithms in simulation and then test them into the real platform with practically no efforts.

As an additional value of the simulator, we are studying its applicability in real-time in order to more precisely evaluate the candidate trajectories generated by the algorithm proposed in D28.6, Section 5.3. The main idea here is to check the admissible configurations of the system with a detailed dynamic model rather than using the footprint of the robot. In this way, we can more precisely determine a safe trajectory.

Last but not least, the simulator can also be useful for training the operators before operating the system in real sewers. In this way the training can be done safely while minimizing risks of doing it with the real platform at its early stages.

5.2 Addition of a new camera

"It is recommended to practice with external cameras or direct sight and implement the learnings in software and/or standard operating procedures to further reduce risk of ending up in unrecoverable situations."

In this section we describe the new camera device that will be installed on top of the robot at the end of the arm as described in Section 4.2.3.

A new inspection camera will be installed in the robot arm located on the top (see Figure 5.3). This small camera allows recording at full HD with a very small footprint. The camera also delivers compressed images at 30Hz, allowing direct forwarding to the operator control station with minimal computation impact to the robot.

Figure 5.3: New camera that will be installed in the arm on top the robot.

The purpose of this new camera is twofold:

- Inspection of the sewer (together with the arm) with high quality imaging. The camera will be used to take snapshots of areas of interest for the operator. Additionally, its installation as end-effector in the robotic arm allows changing the image perspective without moving the robot orientation, simplifying the operation and reducing risks.

- Third-person point of view of the robot for complex maneuvers. This camera also fulfills the function of observing the robot while performing complex or risky operations as fork crossing. The arm allows to point the camera directly to the front or rear wheels, or watching the gutter during risky tasks. Moreover, the camera has a large FOV that will increase the operator awareness when using it with this purpose.

5.3 Improvements in positive obstacle detection

"Dead zones around the robot should be reduced as they are a safety hazard both for robot damage due to collisions, but perhaps more importantly for collisions with personnel in the vicinity of the robot."

We agree with the reviewers that more effort has to be carried out in the proper detection of positive obstacles and, more specifically, slim hanging obstacles. The improvements presented here are motivated by the final demo of Phase II, where the semi-autonomous mode failed to consider a hanging obstacle placed in the middle of the sewer. For this reason, we propose an improvement of the algorithm proposed in D28.6 Section 5.3 that is presented in this section.

The proposed system for safe trajectory generation (STG) relies on the information of the six RGB-D cameras for determining the areas of the floor can be traversed. To this end, the point clouds generated the cameras are processed by a traversability map generator. This

generator fuses the information of all the cameras in the aforementioned map. Figure 5.4 shows the point clouds acquired in the surroundings of the platform at one time. Please note that the point cloud almost completely surrounds the vehicle while the small gap between the robot and the closes part of the clouds is below 20 cm. Figure 5.5 illustrates one of these traversability maps that are used to generate trajectories. Again, the maps provide information in very close areas.
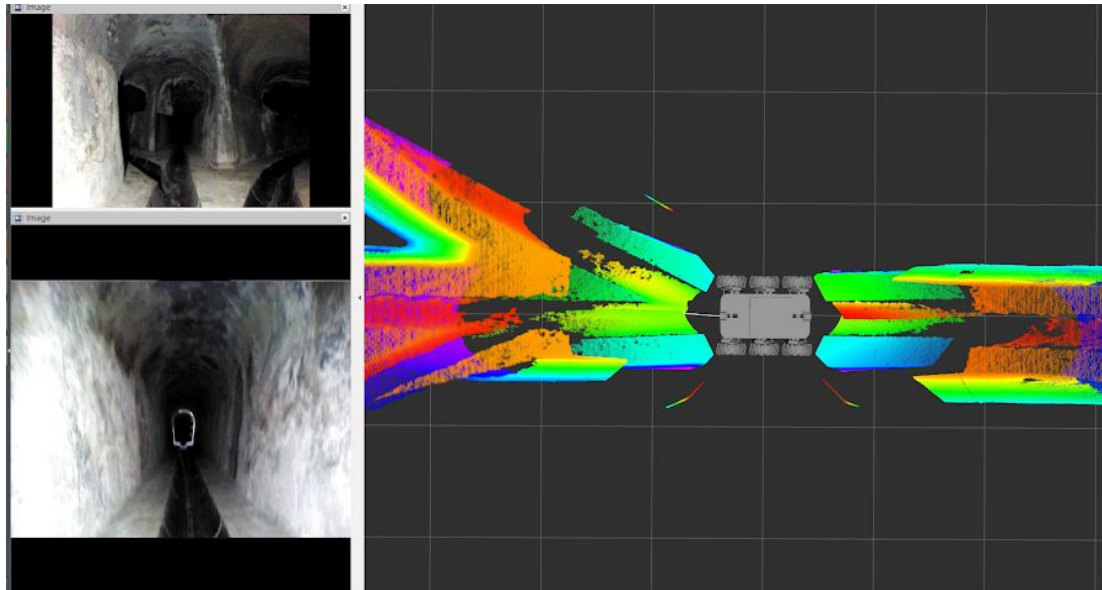

Figure 5.4: (up left) Image from the front camera. (down left) Image from the rear camera (right) Combined point cloud of the six navigation cameras.
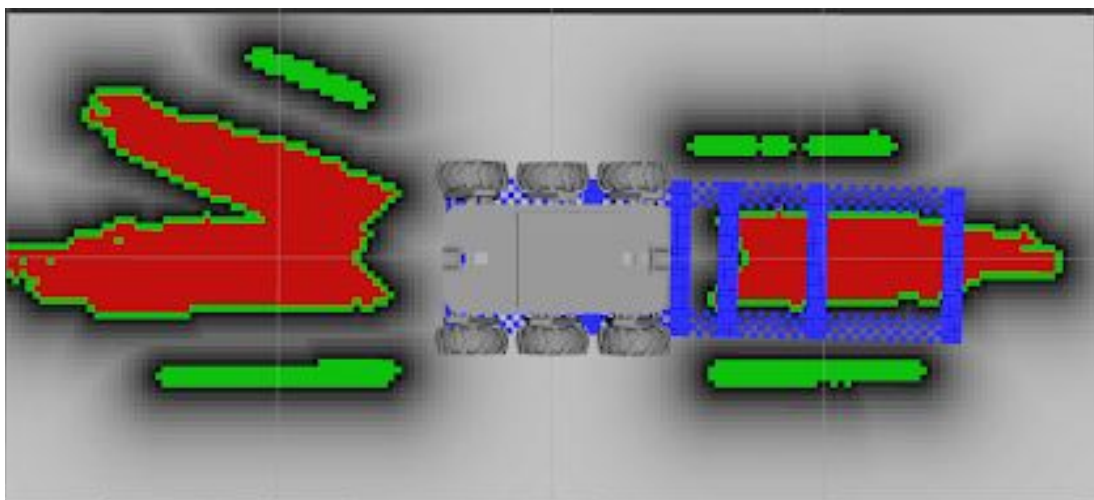

Figure 5.5: Traversability map associated to Figure 5.5. The red areas indicate negative obstacle, the green ones positive obstacles, light gray areas mean no obstacle. The footprint of the generated trajectory is marked in blue.

In the final demo of Phase II, the STG system failed to avoid the collision with a hanging obstacle. The obstacle was very thin (thinner than 5cm) and was placed in the middle of the gutter. After carefully trying to replicate the experiment in our mockup of the sewer we concluded that the failure was due to the following reasons:

- The front and rear cameras did not feed the map generator and the downward pointing cameras were not able to detect the obstacle.

- During the demo the configuration was changed by feeding the front and rear cameras to the map generator. In this case, the system also failed because of the lookahead time of the STG.

- Finally, the map generator was configured to generate a too small map. The map was enlarged in order to prevent collisions with such obstacles from greater distances.

To sum up, we carefully tuned up the whole STG system and the map generator in order to ensure collision free trajectories even in the presence of thin hanging obstacles.

5.4 Safety Procedures

"Safety procedures during the demonstration where insufficient and resulted in people scrambling to get out of the way of the robot on multiple occasions. (sliding wheels, vision of the robot state by operator) It is recommended to practice with external cameras or direct sight and implement the learnings in software and/or standard operating procedures to further reduce risk of ending up in unrecoverable situations."

We would like to mention in this point that we are not completely sure about the situations mentioned here regarding people scrambling to get out of the way of the robot.

We are nevertheless taking some actions. In semi-autonomous mode, the robot will automatically stop if there are obstacles nearby, including persons. The enhancement of the estimation of obstacles surrounding the robot, as described above, will improve thus the safety of persons around.
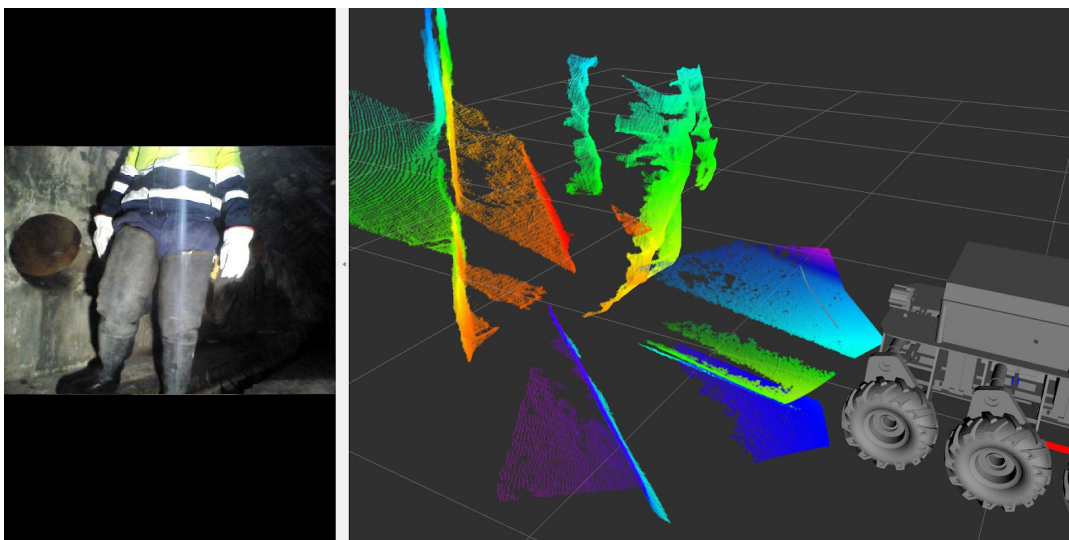

Figure 5.6: Detail of depth information gathered in the presence of one operator. The operator can be detected from more than one meter. If the robot is moving in the direction of the operator, it will automatically stop (semi-autonomous mode).

In fully manual mode the robot is directly controlled by the operator. The new camera and the existing ones will allow the operator to have a more complete view of the surroundings and to determine the presence of persons or obstacles nearby the SIAR platform at any time to avoid such situations.

Furthermore, the final envisaged operational procedure of the SIAR platform makes unnecessary the presence of people nearby the robot once it has been started. Following this procedure, the presence of operators in the surroundings is only required during the deployment, or in a recovery procedure when necessary. In both cases, the SIAR platform will be disallowed to move as a security measure.

Finally, as commented above, we are using now simulations, together with experiments in the mock-up and real experiments to refine all the navigation procedures of the robot.

6. Localization

The system was localized at any time thanks to the implemented localization system that is described in D28.6, Section 5.2. In this section we present an improved version of the localization system that takes profit from common properties of the sewers to acquire knowledge of the relative pose of the robot with respect to the gutter. This local information then can be easily transformed to enhance global localization of the robot by using the GIS provided by BCASA.

6.1 Revision of the localization system

The proposed approach is based on Monte-Carlo Localization, which makes use of a particle filter to represent the robot localization belief. In the proposed filter, each particle represents a hypothesis which consists of a 2D position (x,y) with orientation (ψ). The hypotheses are validated (weighted) according to the position of each particle compared with a topological map obtained from GIS data. In the versions used in Phase II we used the following information to rank the hypotheses:

- Periodically, the deviation from each hypothesis to the sewer graph
- Whenever a manhole was detected, it was used the distance from each hypothesis to its nearest manhole

This method produced good results, but in some cases the set of hypotheses could diverge from the sewer graph and then a relocalization was necessary. This happened twice during the course of Final Demo.

6.2 Relative pose estimation to the gallery

The most common profile of the visitable sewers in Barcelona have in common the existence of two lateral walls that can be easily detected with the depth information of the onboard front and rear cameras of the SIAR platform. In this section, we make use of a fast plane detector in order to detect the lateral walls. Whenever detected, these walls will be used in order to estimate the relative orientation between the robot and the sewer gallery.

We are interested in searching for planar regions in the space that can be modeled as:

$$n \cdot r = d$$

, where **n** is the normal vector, **r** is a point in the plane and **d** is the distance from the origin to the plane. To this end, we use the region-growing based plane detector in order to detect planes in a depth image. This method not only provides us with the estimation of these planar parameters, but also with an estimation of the covariance matrix of the parameters.

Once the planes on the image are detected, the proposed method will try to find large and vertical planar patches in the depth image of the front camera of the robot using the method proposed in the previous section.

Whenever two large enough vertical planes are found, they are used in order to estimate the relative angle of the walls with respect to the robot. As thousands of pixels are used for the estimation, the estimation of the planes is accurate enough to be used for precisely estimating the orientation of the walls with respect to the robot. This relative angle will be used to rank the hypotheses according to the available GIS information from local authorities.

The idea is to intersect the one of the wall planes (P) with the floor plane (G). For the sake of clarity we assume that the calculations are carried out in a gyro-stabilized frame centered in the base of the robot, where k is the unit vector along the z axis.

$$P \equiv \{ \boldsymbol{n} \cdot \boldsymbol{r} = d \}$$
$$G \equiv \{ \boldsymbol{k} \cdot \boldsymbol{r} = 0 \}$$

Then, the relative orientation between the gallery and the can be estimated by obtaining the intersection intersection between P and G. This can be done as follows:

$$\boldsymbol{l} = \boldsymbol{n} \times \boldsymbol{k}$$
$$\theta = arctg \left(\frac{l_y}{l_x} \right)$$

, where θ is the relative orientation.

Once the relative angle is known, it is compared with the relative orientation of the robot with the gallery. This relative orientation can be calculated if we know which is the gallery the robot is traversing and with the aid of GIS. The procedure starts by searching the closest gallery to the current hypothesis. Then, we calculate the relative orientation (θ_r) of the gallery with the orientation of the hypothesis and the global orientation of the gallery. Finally, the weight of the hypothesis is calculated taking into account the difference between the relative orientation of the hypothesis θ_r and the relative orientation obtained with the proposed method θ .

6.3 Experimental results

In this section we compare the method proposed in this section with the one used in Phase II and during the final Demo. The results have been taken from the data gathered in a experiment on October 21st, 2017. Figure 6.1 represents the localization error measured whenever the platform passed below a manhole. Due to the stochastic nature of the localization algorithm, the distribution of the error over 50 runs is represented.

In comparison, the proposed method is able to reduce the median error in almost all cases. In addition, the distribution of errors present lower dispersion when using the estimation of the relative orientation with the sewer.
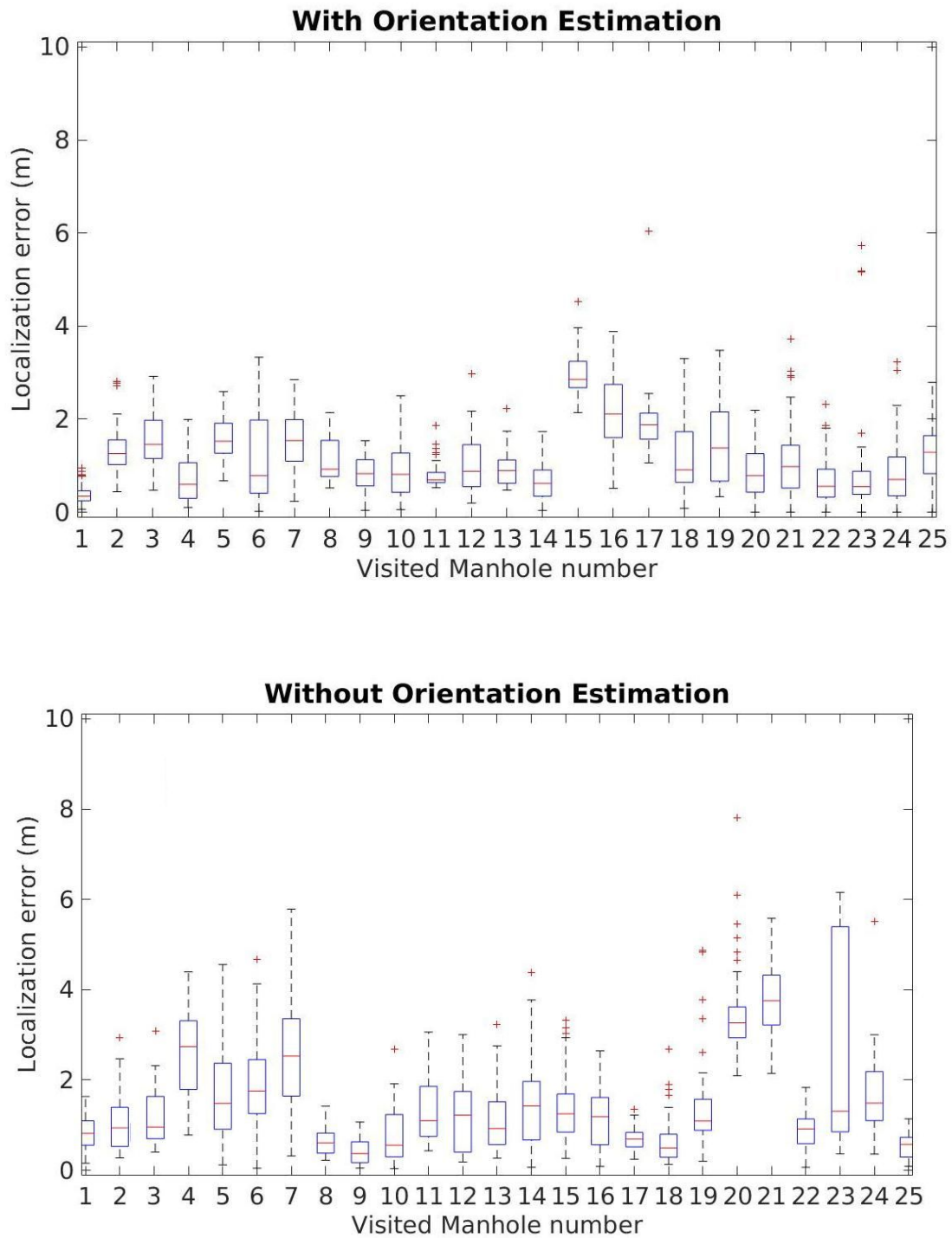
Figure 6.1: Distribution of errors when passing below the manholes in localization experiments. With orientation estimation (up) and without orientation estimation (down)

7. Inspection

"The consortium has made commendable progress, but this area still needs improvement. The consortium should take due note of the reporting requirements as outlined in the challenge brief and should interact as much as possible with end users to understand the inspection and reporting requirements. This pertains for instance to the defect recognition and classification and reporting in the map."

As commented in Section 2, during the demo we already included an initial version of automatic serviceability inspection capabilities, even though the associated KPIs were planned for Phase III.

The display of these preliminary results was not fully compliant with the specific format as indicated in the Challenge Brief, but the required information to comply with such format is already available, and steps are being carried out to do it.

As an example, regarding the "Serviceability Reduction Alarm", the Challenge Brief mentions:

"On the basis of the scanning or the video made, the robot has to compare the obtained data with the available information of the sewers (mainly type and section) and identify where the sewer serviceability has been reduced. The operator should receive a "pop-up" alarm that indicates the location of the obstruction and helps to decide if the robot has to make an extra specific snapshot or video."

In the demo, the robot applied the mentioned procedure and was able, in real-time, to recognize the section type and using this information compare the 3D data to detect the potential obstructions and overlay them on the image using colours. This can be seen in Fig. 7.1.
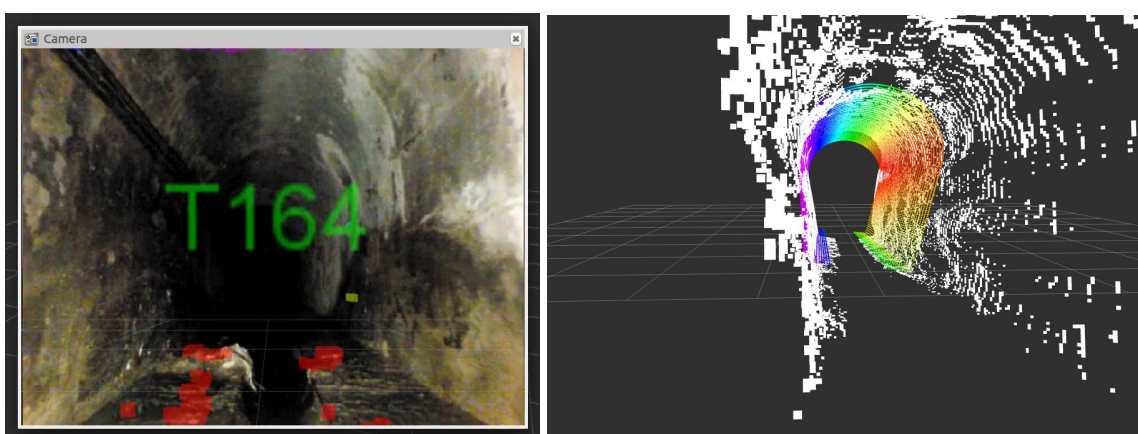

Figure 7.1: Left: automatic detection of section type (T164) overlayed on the image. Right: comparison of sensor 3D data (white) with detected section model (colour). The potential reduction on the serviceability is marked with red colour in the left image. This information can be used to raise alarms for the operator.

The operator was able to see this information in the Control Station, but in a separated screen. We are working on the generation of alarms for the operator in the new version of the Control Station as indicated.

Regarding the "Structural Defects Inspection", the Challenge Brief indicates:

"The prototype should locate and identify critical damage inside the sewers, whether it is located on floor (sewer's bottom), vault (sewer's roof) or walls.

Identification of critical defects should be done according to the table below [...]

Defects location should be stated giving the following measurements:
- Distance from the nearest manhole to the defect: nodes (manholes and inlets) are codified in the GIS.
- Circular location following clock-face pattern (12-above, 3-right hand, 6-below, 9-left hand)."

During Phase II, we were also able to highlight potential structural defects in real-time and locate them in 3D (see Fig. 7.2). As the robot is localized with respect to the GIS (Section 6), it was possible to locate the defects in global coordinates, as shown in Section 2. We have been working to include the defects on the map (see Fig. 2.1). And it is thus also possible to indicate the location of the damage with respect to the closest manhole. This information will be included in the next version of the system.
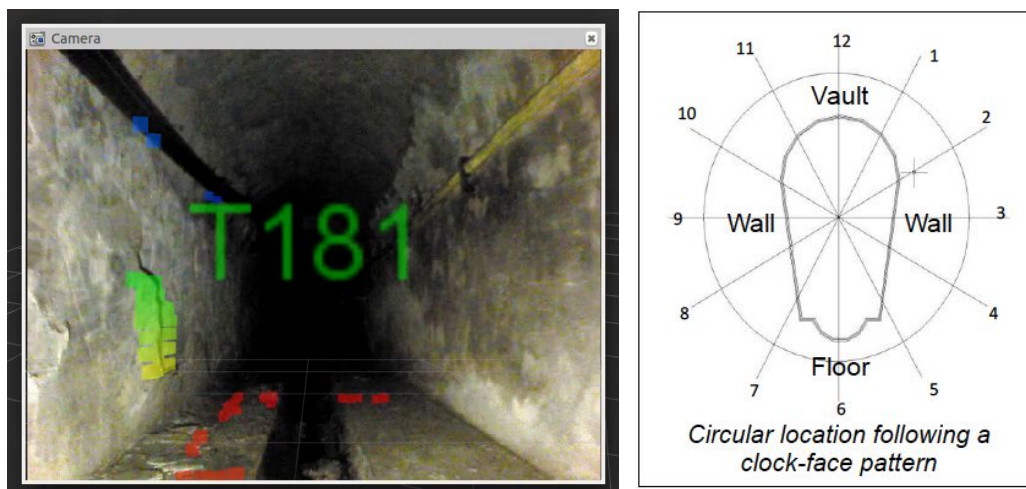
Figure 7.2: Left: automatic detection of section type (T164) overlayed on the image and potential structural defects (a potential break with some losses). The information is provided in 3D, so it is possible to indicate the location of the potential defect according to the clock-face pattern indicated in the Challenge Brief (right). Given the localization of the robot, it is also possible to localize the defect on the map (see Fig. 2.1).

The defects currently are not classified automatically according to the Challenge Brief options (Cracks, Fractures, Breaks, Breaks with Loss and Collapses), but the operator can manually select the type of defect if an alarm is raised.

Besides the inclusion of the information in the new Control Station, one of the main objectives is to reduce the potential number of false alarms.

We have also arranged a meeting with the end-user BCASA to further verify and clarify the requirements related to the inspection modules.

"A more robust way to do measurements on dimensions and distances should be implemented. Visual data is acceptable by end users and, 3D reconstruction is adequate."

As commented, the system is able to provide 3D reconstructions. Using the 3D data it is possible to make measurements on dimensions and distances, but during the demo we did not have any specific tool for that. We are working on tools for measuring distances in the Control Station. It is tricky to adequately do so using a 2D representation, and we will include references, as the own model of the robot and grids (see Fig. 7.3), to help in the process of measurement.
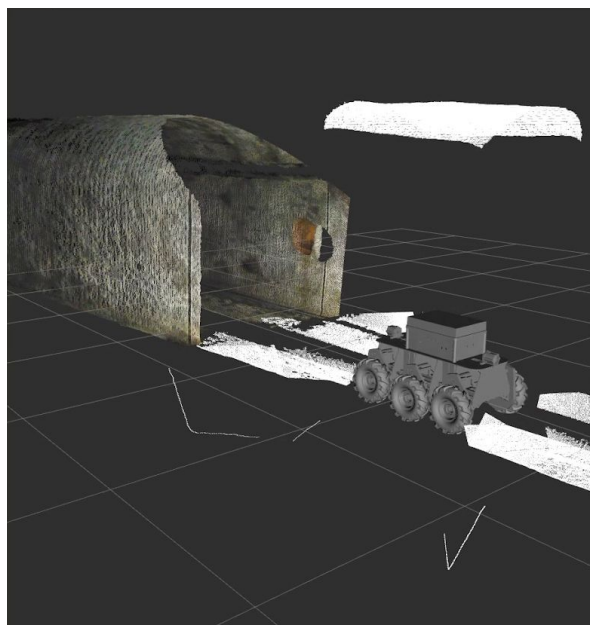

Figure 7.3: The 3D information provided by the robot can be used by the operator to perform distance measurements. The robot model and grids (in the view each square represents 1 square meters) will help in the process.

8. Conclusion

As previously presented, the SIAR team has directly addressed the reviewers recommendations since the Phase II final demo. Other actions have been also implemented in order to increase the reliability and robustness of the SIAR robot, both hardware and software.

While some of the solutions presented are already concluded, some others are still in development given the high complexity and time consuming nature of certain tasks as robot frame redesigning or autonomous navigation improvements.

Next months will be devoted to finish the pending actions and to test in Barcelona the different improvements we have been developing in the first period of the Phase III. Several experiments will be performed in order to evaluate the improvement in robot navigation, the new robot frame and its new components, and the new communication system.